Spacecraft Trajectory Planning and Execution for the MESSENGER Mission

James V. McAdams, Christopher G. Bryan, Stewart S. Bushman, Carl S. Engelbrecht, Sarah H. Flanigan, and T. Adrian Hill

ABSTRACT

The spacecraft trajectory and the associated course-correction maneuvers provided a primary means for accomplishment of the scientific objectives of the MErcury Surface, Space ENvironment, GEochemistry, and Ranging (MESSENGER) mission. Whereas other articles in this issue offer a quantitative performance assessment of MESSENGER's course-correction maneuvers, this account identifies unique aspects and lessons learned from the examination of the processes and team interactions for maneuver design through maneuver reconstruction at the core of this successful NASA mission. Keys to mission success included forward thinking in the creative use of maneuvers as a means of preparing for future important maneuvers, as well as exercising flexibility to allow change from the nominal plan when this change would either increase scientific return or enable new scientific observations to answer questions that arose during the mission. Cautious use of propellant reserves and a willingness to accept higher risk near the end of flight operations enabled a 3.1-year extension of the yearlong orbital phase of the primary mission.

INTRODUCTION

Although the MErcury Surface, Space ENvironment, GEochemistry, and Ranging (MESSENGER) mission relied on six planetary gravity-assist flybys to impart >91% of the trajectory's total velocity change (ΔV), 42 trajectory-correction maneuvers (TCMs) and orbit-correction maneuvers (OCMs) directed the 10.8-year mission on a course that met or exceeded all primary and extended-mission scientific objectives. The dual-mode monopropellant–bipropellant propulsion system fully utilized onboard propellant via many maneuver implementation variations. Mission planners often demonstrated a willingness to explore, understand, and apply new information as maneuvers were designed, executed, and evaluated. Maneuver design and implemen-

tation strategies evolved on the basis of lessons learned and results from in-flight subsystem resource-utilization studies, such as propellant fluid dynamics analyses in mostly empty fuel tanks. Notable MESSENGER TCMs with characteristics shared by no other spacecraft mission appear in Table 1.

Propulsive maneuvers for MESSENGER can be classified by trajectory change, mission phase, or propulsive mode. Trajectory-change maneuvers and their associated mission phases include deep-space maneuvers (DSMs) that adjusted for imperfect planet position phasing between cruise-phase planetary encounters, statistical TCMs that cleaned up DSM execution errors and off-target planetary flybys during the cruise phase,

Table 1. Spacecraft mission firsts for MESSENGER course-correction maneuvers

Maneuver Name	Date (UTC) Implemented	Mission-Unique Characteristic
MOI	18 Mar 2011	First time any spacecraft completed an MOI maneuver
OCM-12	21 Jan 2015	Closest propulsive maneuver to the Sun (30.4795% of average Earth–Sun distance)
OCM-15A	8 Apr 2015	First course-correction maneuver to rely solely on GHe pressurant

Mercury orbit insertion (MOI), and OCMs that changed minimum altitude relative to Mercury or adjusted orbit period during the Mercury orbital phase. The propulsive mode identifies the active thruster sets for both primary ΔV implementation and spacecraft attitude control, the propellant type(s) and sources, the maneuver complexity (the number of segments with a different primary thruster set or a different fuel tank source), and the attainable thrust level. Mode-1 maneuvers drew hydrazine from a small, pressurized auxiliary tank for small maneuvers (<10 m/s ΔV) by using one propulsive segment with a subset of the 12 smallest (4.4 N) thrusters. The monopropellant mode-2 and bipropellant mode-3 maneuvers used propellant from one or both of the main fuel tanks and had multiple thrust-imparting segments to maximize propellant usage efficiency and to shift propellant to ensure uninterrupted thrust throughout the maneuver. Main-burn segment primary thrusters included the four 22-N monopropellant thrusters for mode-2 maneuvers and the 672-N Leros-1b main engine thruster (LVA for "large velocity adjust") for mode-3 maneuvers. Approximately 90% of total ΔV imparted to the spacecraft via the propulsion subsystem came during the mode-3 (>20 m/s ΔV) maneuvers; these maneuvers were the most efficient because they imparted the most ΔV per kilogram of propellant. Each maneuver concluded with a tweak segment that maintained spacecraft attitude control with near-zero ΔV imparted to the spacecraft until propellant slosh and structural component oscillation were damped.

The life cycle of each course-correction maneuver from design to final evaluation (reconstruc-

tion) began with maneuver trades during trajectory optimization by the mission design team at the Johns Hopkins University Applied Physics Laboratory (APL) and ended with a final maneuver reconstruction report from the navigation team at KinetX Aerospace. The maneuver design-to-implementation process included occasional practices of key maneuver types, independent design verification, reviews, testing, and multiple maneuver command-sequence upload opportunities.
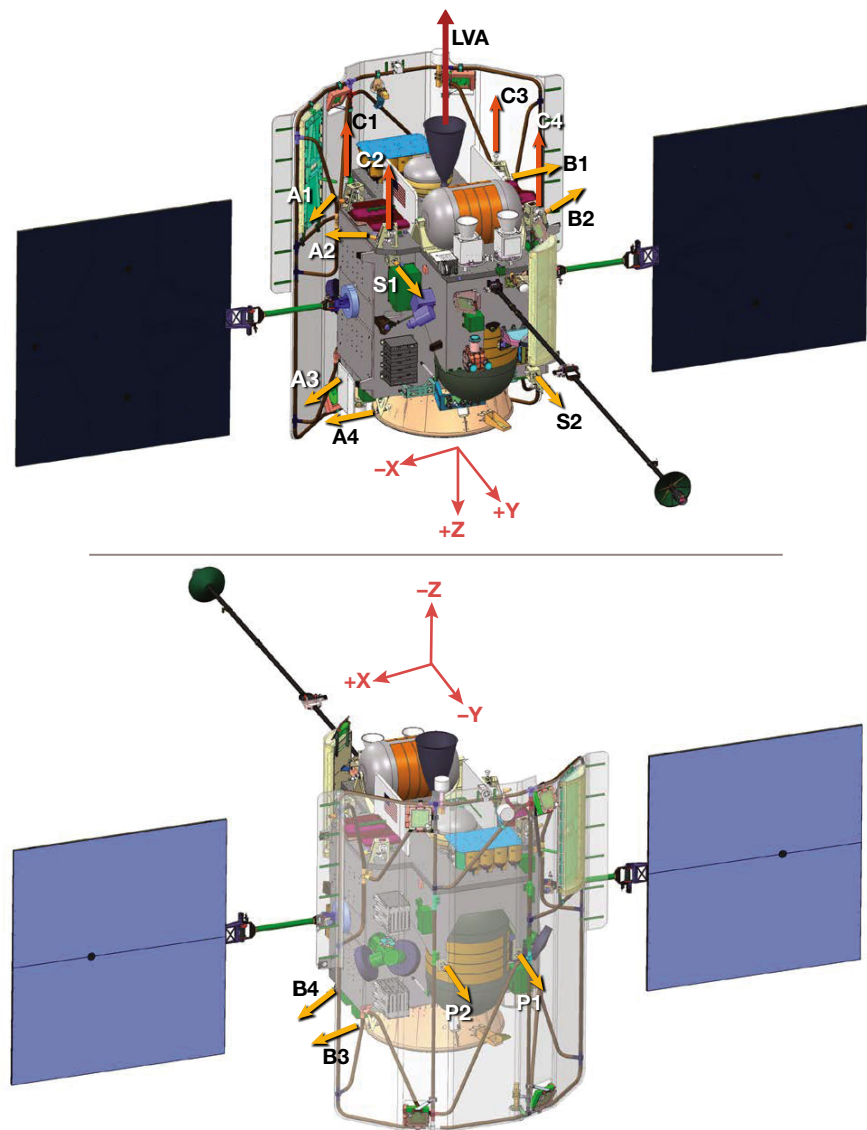
Figure 1. MESSENGER thruster locations and exhaust vector directions.

The MESSENGER team benefited from MESSENGER project office and NASA leadership that allowed the engineering team to develop and implement alternative maneuver strategies that were not defined before launch. Alternative maneuver strategies included either splitting planned TCMs into multiple parts or turning the spacecraft along a thrust direction profile to test key aspects of the mission-critical MOI maneuver. New propellant management recommendations from an independent expert contractor led to improved propulsion system performance during MESSENGER's extended mission.

The mission's most important propulsive event, MOI, benefited from years of preparation that focused on lowering risk at this transition from the interplanetary cruise phase to the Mercury orbital phase. Many improvements and even an alteration in the primary science orbit definition were made between launch and MOI. After MOI execution, the best available estimate of the Mercury arrival aimpoint, MOI maneuver performance, and initial orbit characteristics indicated a successful maneuver that required no cleanup.

PROPULSION SYSTEM OVERVIEW

The high ΔV requirement of the MESSENGER mission necessitated a mass-efficient propulsion system design. The MESSENGER propulsion system was a lightweight, pressurized, dual-mode bipropellant system designed and built by Aerojet Rocketdyne.[1] Figure 1 identifies the thrusters and exhaust vector directions. A Moog-ISP bipropellant Leros-1b, denoted as the LVA engine, provided large ΔV capability.[1–3] The C thrusters were Aerojet Rocketdyne 22-N (5 lb_f) MR-106Es, and the A, B, S, and P thrusters were Aerojet Rocketdyne 4.4-N (1 lb_f) MR-111Cs. To provide redundant three-axis attitude control, the A and B thrusters were arranged in double-canted sets of four. Both S thrusters provided sunward ΔV, and both P thrusters provided anti-sunward ΔV.

Propulsive maneuvers included commanded momentum dumps, TCMs, DSMs, and OCMs. The MESSENGER propulsion system provided >2213 m/s of propulsive ΔV, including 4.7 m/s delivered before impact using gaseous helium (GHe) pressurant as cold gas propellant.

Hydrazine (N_2H_4) and nitrogen tetroxide (N_2O_4) were stored in three identical main tanks—two fuel tanks (FT1 and FT2) and one oxidizer tank—and also in a fourth refillable auxil-

Table 2. Liquid propellant load at BOL and EOL

Tank	BOL Load Before Launch	EOL Load Before Impact
AUX	9.34 kg N_2H_4	0 kg N_2H_4
FT1	178.0 kg N_2H_4	<0.1 kg N_2H_4
FT2	178.0 kg N_2H_4	1.6 kg[a] N_2H_4
Oxidizer	231.6 kg N_2O_4	1.9 kg N_2O_4

[a] Believed trapped in baffles; 0 kg accessible

iary fuel tank (AUX). GHe was stored in a single pressurant tank. The AUX used an elastomeric diaphragm for positive propellant expulsion, and the propellant in the main tanks was expelled, usually after settling force was provided by thrusters fed from the AUX, using the helium pressurization system. Each main tank contained a vortex suppressor to stabilize flow at the outlet and two annular baffles designed to inhibit propellant slosh during launch.[2–4] Table 2 shows the tank liquid propellant loads at beginning of life (BOL) and end of life (EOL).

LIFE CYCLE OF A MANEUVER

Maneuver Design to Implementation

The MESSENGER maneuver design process relied on cooperative and effective interaction within the flight team. Depicted in Fig. 2, this process began with the navigation team processing spacecraft orbit data and releasing an updated ephemeris for a recently completed portion of the spacecraft trajectory and a prediction of that trajectory until shortly after the next scheduled TCM. Navigation personnel and mission design personnel worked together to design and independently verify
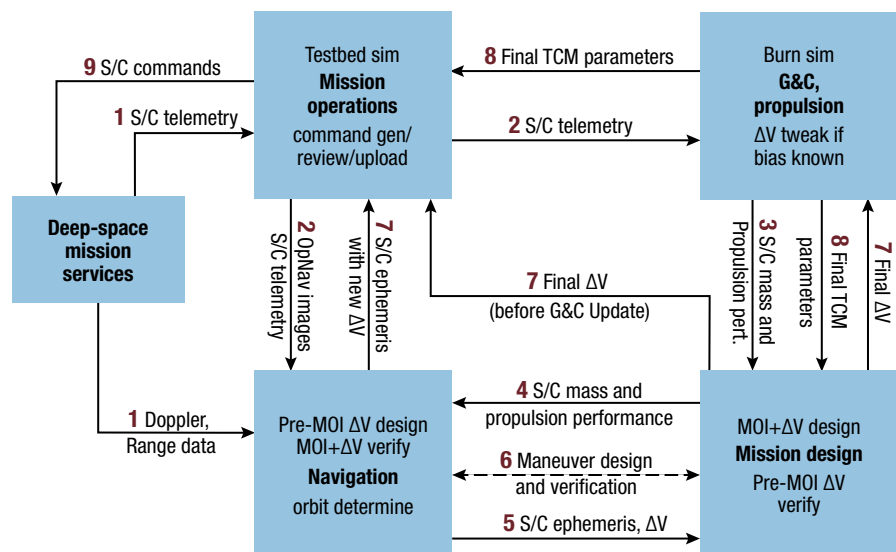

Figure 2. Maneuver design team interfaces and data flow. Gen, generation; OpNav, optical navigation; Perf., performance; S/C, spacecraft; Sim, simulation.

that all maneuvers met predefined TCM conversion criteria. For the 5.2 years before the final design of DSM-5 (the final TCM before MOI), the navigation team provided the maneuver (ΔV) design implemented on the spacecraft and the mission design team provided an independent maneuver design verification. For the next 5.4 years (from MOI design through OCM-18 design), these roles were reversed: the final maneuver design that was implemented came from the mission design team and was verified by the navigation team. After receiving the final TCM design and the estimated spacecraft orientation at the start of propulsive thrust, the guidance and control (G&C) team modeled TCM performance via Monte Carlo analyses that varied parameters such as center of gravity (influenced by propellant amount and location) and set TCM parameters to minimize spacecraft risk and maximize TCM accuracy. A spacecraft autonomy expert worked with G&C and mission operations personnel to set spacecraft checks before and during the TCM to ensure safe maneuver completion. The mission operations team then completed TCM design by running spacecraft test-bed simulations for nominal and abort maneuver scenarios, generating and uploading to the spacecraft the maneuver command sequence. Most TCM process steps were repeated and reviewed for both the preliminary and final TCM designs, with the final TCM design based on additional spacecraft orbit data and, on rare occasions, some alteration in one or more aspects of how the maneuver would be implemented. During TCM implementation, the flight team assembled in the Mission Operations Control Center, monitored progression of the TCM command sequence, prepared a quick-look preliminary TCM performance assessment, and determined whether any follow-up contingency plan needed to be initiated.

Maneuver Design and Verification

After selection of the TCM propulsive mode (see the Maneuver Planning and Implementation section), the spacecraft trajectory optimization and maneuver design process accounted for many other design constraints and requirements. The TCM design began with trajectory optimization, which accounted for minimum-altitude constraints of 200 km at each Mercury flyby and at Mercury arrival and 300 km at each Venus flyby, as well as factors affecting TCM placement. Large cruise-phase maneuvers were placed such that light-time-delayed, real-time monitoring was used from one or more Deep Space Network (DSN) ground stations. The best example of changing maneuver timing to enhance mission success involved moving DSM-2 more than 2 weeks earlier than its minimum-ΔV location, a shift that enabled real-time monitoring of DSM-2 outside a region of communications interference from the Sun known as a superior solar conjunction. This DSM-2 shift to an earlier

time also enabled 7-day no-propellant-cost and 13-day last-resort-backup options before a 40-day period with either unreliable or no communication possible with the spacecraft. Delaying DSM-2 until after the solar conjunction would have eliminated the potential for MOI because the long delay would introduce a violation of a key spacecraft attitude constraint for TCMs performed close to the Sun. For maneuvers that were less mission-critical than DSM-2, maneuver contingency planning involved designing and testing a backup maneuver ~1 day after the planned maneuver and preparing a strategy with later contingency options before the next trajectory-altering event. Before the higher-risk final month of the mission, no maneuver contingency plan was ever implemented.

Additional maneuver design factors involved either the Sun-relative or Earth-relative orientation of spacecraft components such as the ceramic-cloth-covered sunshade or spacecraft antennas. The vast majority of maneuvers were sufficiently close to the Sun to require sunshade thermal protection of the spacecraft bus. All such maneuvers require alignment of the surface normal to the sunshade's center panel to within 12° of the spacecraft–Sun direction; this requirement is the core aspect of MESSENGER's Sun keep-in (SKI) constraint. Compliance with the SKI constraint limited placement of medium-ΔV and large-ΔV cruise-phase maneuvers to near perihelion or aphelion and limited placement of medium and large ΔV Mercury orbital-phase maneuvers to near the dawn–dusk orientation of the spacecraft orbit's line of nodes (when the spacecraft–Mercury–Sun angle is close to 90° as the spacecraft crosses Mercury's equator). Another maneuver attitude constraint involved turning the spacecraft to orient Earth near the boresight of either of two medium-gain fanbeam antennas. These were mounted on the Sun-facing side of the sunshade and the anti-Sun spacecraft deck.

After completing primary and contingency maneuver designs, the lead maneuver design team sent the maneuver verification team a maneuver interface file, consisting of a maneuver summary and associated propulsive performance data. Propulsive performance data in the maneuver interface file included (for each maneuver segment) start time, ΔV magnitude, duration, thrust direction and magnitude, and mass flow rate. The maneuver interface file also included values of maneuver target parameters that specified the aimpoint at the next planetary encounter or Mercury-relative spacecraft orbit parameters. The maneuver interface file was used in design verification, which consisted of modeling the maneuver performance parameters in the trajectory and determining whether the maneuver target parameters from the two independent software suites matched within some small tolerance. Small differences between target parameters as determined by the mission design and navigation teams were expected, and these were

often due to minor variations in force modeling implementations[5] between the two independent systems.

Maneuver Planning and Implementation

G&C software recognized mode-1, -2, and -3 propulsive maneuver types, which were defined by the active thrusters and the source propellant tanks. On the basis of the desired ΔV and the best estimate of remaining propellant, the mission design and G&C teams coordinated early in the maneuver design process to identify the maneuver's propulsive mode.

Mode-1 maneuvers were used for small-ΔV (<10 m/s) and momentum off-loading maneuvers using either the 4.4-N or the 22-N thrusters, with fuel supplied by the AUX operating in blow-down mode. The G&C software divided each mode-1 maneuver into main and tweak segments. The mode-1 main thrust segment is the only segment during which ΔV was imparted to the spacecraft. The maneuver cleanup tweak segment followed the thrust segment, during which the attitude-control thrusters would fire until structural excitations and propellant slosh were sufficiently damped out to return control to the reaction wheels.

Mode-2 maneuvers were selected for medium-ΔV (10–25 m/s) maneuvers using the 4.4-N and 22-N thrusters. The G&C software divided each mode-2 maneuver into three segments: settle, main, and tweak. The settle segment executed a "settling burn" with fuel from the AUX used in blow-down mode in order to prepare the main fuel tanks for the main segment. During the main segment, the thrusters were pressure-fed from the main fuel tanks, and the majority of the target ΔV was imparted. At main segment start, the AUX was refilled from a main fuel tank. During a closed-loop controlled maneuver, the main segment continued until either the target ΔV was attained or the maneuver reached a duration limit. The tweak segment followed, using fuel supplied by the AUX.

Mode-3 maneuvers, employed for large-ΔV (>25 m/s) maneuvers, used the LVA thruster as the primary source of ΔV. The G&C software divided mode-3 maneuvers into five segments: settle, refill, main, trim, and tweak.

Although the mode-3 settle and tweak segments were the same as those used in mode-2 maneuvers, a segment was added to refill the AUX. This refill segment was required because during the main segment the main fuel tanks were unable to support the flow rate required to fire simultaneously the LVA thruster for primary ΔV and the C thrusters for attitude control while also refilling the AUX. In the main segment, the LVA thruster fired for an integral number of seconds using propellant from the oxidizer and main fuel tanks. At a predetermined time (in an open-loop controlled maneuver) or when a percentage of total ΔV was reached, as determined from accelerometer data (in a closed-loop controlled maneuver), the G&C subsystem transitioned to the trim segment. The trim segment used monopropellant thrusters and fuel from the main fuel tanks to complete the desired ΔV.

In addition to propulsive mode, details such as segment durations, active thruster sets, thruster control parameters, and fuel tank switching schemes were selected for each maneuver. Most maneuvers were performed as closed loop, using high-rate accelerometer data to guide the maneuver and minimize maneuver execution errors. Segment durations were chosen to balance maneuver efficiency with specialized propulsion system operational guidelines, such as those levied on the MESSENGER propulsion system after MOI to maximize propellant accessibility. Table 3 provides details of the maneuver segments associated with OCM-3. The LVA thruster fired for only 13 s to ensure that the trim segment would last at least 61 s. For post-MOI LVA maneuvers, the trim segment provided a "soft landing" to stabilize propellant after LVA thruster shutoff. For each maneuver segment, thruster sets were identified as either imparting ΔV or providing attitude control. Thruster pulsing schemes were chosen to improve maneuver efficiency. For instance, when the C thrusters were selected to impart ΔV, they were usually off-pulsed (close to 100% duty cycle) for attitude control in order to minimize the pulsing required from the A and B thrusters, which contributed ΔV away from the desired direction because of their off-thrust-axis alignment. For every

Table 3. OCM-3 sequence thruster activity summary (attitude-control thrusters on-pulsed as needed)

Maneuver Segment	Designed Duration (s)	Achieved Duration (s)	ΔV Thrusters	Attitude-Control Thrusters	Fuel Tanks
Settle	60	60	A1, A2, B1, B2 (continuous)	A3, A4, B3, B4, C2, C3	AUX
Refill	23	23	C1, C4 (off-pulse)	A3, A4, B3, B4, C2, C3	FT1
Main	12	13	LVA (continuous)	A1, A2, B1, B2, C1–C4	Balance portion (5 s) with FT1, then alternate every 20 s
Trim	76.8	69.5	C1, C4 (off-pulse)	A1, A2, B1, B2, C2, C3	Continue to alternate tank source every 20 s
Tweak	30	30	None	A1–A4, B1–B4	AUX

maneuver, high-fidelity simulations were run to ensure that the thruster control parameters would not only minimize maneuver execution errors within acceptable propellant usage ranges but also maintain sufficient margin relative to the SKI limits. The fuel tank switching scheme was chosen to limit center-of-mass movement and avoid excessive thruster duty cycling.

The G&C onboard software provided internal maneuver fault-protection checks, which monitor system conditions at burn ignition ("initiation" checks) and throughout the maneuver ("abort" checks). After initiation check failure, the spacecraft remained in operational mode with the maneuver start on hold. When an abort check failed, the maneuver ended in a controlled manner and the G&C software raised a mode demotion request flag to the fault-protection processor (FPP). Each maneuver mode has a set of initiation and abort checks. The complete maneuver design included selecting the internal maneuver fault protection (e.g., which initiation and abort checks to enable, which limits to check, how to set activation times relative to burn ignition, and how long qualifying abort conditions should persist). Table 4 lists the initiation and abort checks available in the G&C software for each maneuver mode.

Table 4. G&C maneuver initiation and abort checks available for each maneuver mode type

Initiation/Abort Check Failure Conditions	Mode 1 Initiation	Mode 1 Abort	Mode 2 Initiation	Mode 2 Abort	Mode 3 Initiation	Mode 3 Abort
Spacecraft not in operational mode	available	available	available	available	available	available
Inertial measurement unit problem or invalid accelerometer data	available	available	available	available	available	available
Attitude error too high or no attitude knowledge	available	available	available	available	available	available
Required thrusters unavailable	available	unavailable	available	unavailable	available	unavailable
ΔV thruster set inconsistent with desired inertial ΔV direction	available	unavailable	available	unavailable	available	unavailable
Error between accumulated ΔV and onboard reference too high	unavailable	available	unavailable	available	unavailable	available
C thruster thrust too low	unavailable	available	unavailable	available	unavailable	available
C thruster duty cycle too high	unavailable	available	unavailable	available	unavailable	available
LVA thrust too low	unavailable	available	unavailable	available	unavailable	available
Latch valve over-current condition	unavailable	available	unavailable	available	unavailable	available
Fuel feed pressure too low	unavailable	available	unavailable	available	unavailable	available
Fuel line bleed-in not completed	available	unavailable	available	unavailable	available	unavailable
AUX pressure too low	unavailable	available	unavailable	available	unavailable	available
Main tank pressures out of range	unavailable	available	unavailable	available	unavailable	available
Regulator pressures too high	unavailable	available	unavailable	available	unavailable	available
Oxidizer tank and main fuel tank pressure differential too high	unavailable	available	unavailable	available	unavailable	available
LVA fuel latch valve closed	unavailable	available	unavailable	available	unavailable	available
LVA manifold pressure out of range	unavailable	available	unavailable	available	unavailable	available
LVA flange temperature too low	unavailable	available	unavailable	available	unavailable	available

White, available; gray, unavailable.

Maneuver Monitoring and Reconstruction

The primary maneuver reconstruction product generated by the G&C team and supplied to the navigation and mission design teams was the small forces file. The small forces file listed accumulated ΔV in the EME2000 (Earth Mean Equator of 1 January 2000) reference frame, spacecraft attitude quaternions, cumulative thruster-on time for each thruster, and total (propellant) mass decrement throughout the maneuver. All accumulated values were relative to the burn start time. High-rate (100 Hz) accelerometer data helped compute the accumulated ΔV values. Estimated total mass decrement was based on start mass, thruster mass flow rates, and cumulative thruster-on times.

Although the small forces file contained all data from the G&C team necessary to enable maneuver reconstructions by both the navigation and mission design teams, the data were presented in additional formats to enable further evaluation of maneuver performance. For instance, the comparison between effective thrust and expected thrust, which accounts for duty cycles, helped identify off-nominal propulsion system performance such as gas ingestion. In Fig. 3, which shows OCM-3 performance, gas ingestion in the oxidizer tank is evident ~5 s into the LVA segment, when a 75-N drop in effective thrust was inconsistent with the expected thrust. After detailed review of effective thrust and thruster duty cycles, the maneuver attitude error was analyzed to ensure control authority and sufficient margin from SKI limits.

The mission design team supported maneuver monitoring by applying telemetry-based maneuver performance estimates from the G&C and propulsion teams
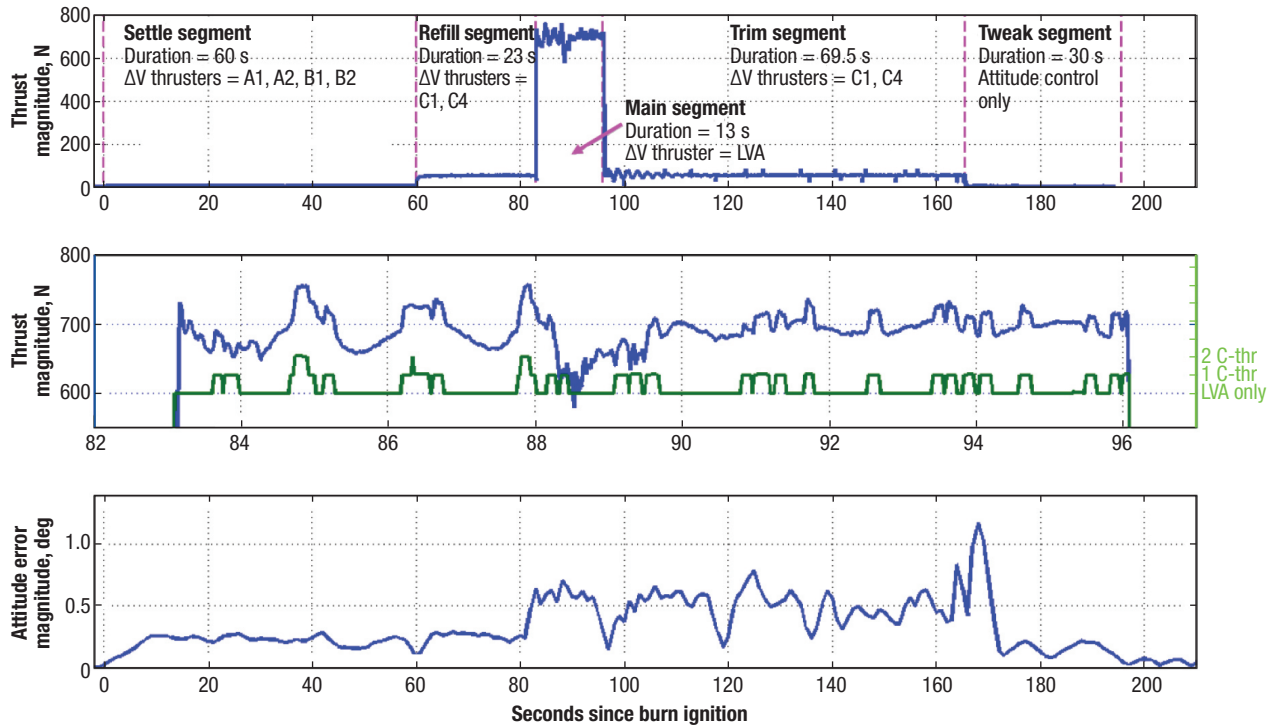
Figure 3. OCM-3 flight performance for (top) full-maneuver thrust magnitude (middle, left axis) LVA-segment-only thrust magnitude, and (middle, right axis) expected thrust profile based on LVA and C thruster duty cycles as well as (bottom) estimated attitude error magnitude.

to provide a basis for estimating how far the spacecraft would deviate from the maneuver's orbit target parameters. Before MOI these maneuver target parameters were specified as closest approach time and spacecraft location at closest approach of the next planetary encounter, either one of the six planetary flybys or Mercury arrival for MOI. After MOI these target parameters were associated with an orbit minimum altitude (periapsis) point shortly before the next scheduled maneuver except for two OCMs early in 2012 that had no firm date set for the next OCM. For quick-look orbit-phase maneuver performance assessment meetings hours after OCM execution, the mission design and navigation teams provided spacecraft orbit parameter updates in order to help the mission operations team shift spacecraft event times within the next opportunity to update the "zero TCM execution error" baselined command load sequence.

The navigation team played a key role in maneuver execution monitoring. Before maneuver execution, the team estimated the 3-standard-deviation, two-way Doppler residual uncertainty envelope before, during, and after the burn based on several factors, including propagated trajectory uncertainties, maneuver error assumptions by the G&C team, and the look angle between the Earth line-of-sight to the spacecraft and the burn direction. Trajectory predictions including the nominal burn were sent to the DSN before the burn. Burn exe-

cution was monitored in real time, and actual Doppler residuals were plotted and compared with the predicted uncertainty envelope. Figure 4 shows an OCM-3 Doppler residual plot (in hertz), which was executed early in the mission's orbital phase on 7 September 2011. With the nominal burn modeled in the trajectory that produced the residuals, observation that the pre-OCM residual was close to the post-OCM residual indicated a high likelihood of accurate (nominal) burn execution. As shown in Fig. 4, the observed Doppler residuals were well within the predicted uncertainty envelope, which indicated nominal maneuver performance for OCM-3.

After every maneuver execution, the navigation team reconstructed actual maneuver performance from post-maneuver radiometric tracking data. Accurate estimation of actual maneuver performance relied on optimal observation and force modeling. During the interplanetary cruise phase, the navigation team processed three radiometric tracking data types: Doppler, range, and delta-differential one-way ranging. The navigation team corrected the Doppler data for the effects of orientation changes during a DSN tracking pass (motion of the spacecraft antenna phase center relative to the spacecraft center of mass). During the Mercury orbital phase, delta-differential one-way ranging data were not required.

For the mission's orbital phase, the navigation team implemented several force models specific to the Mer-
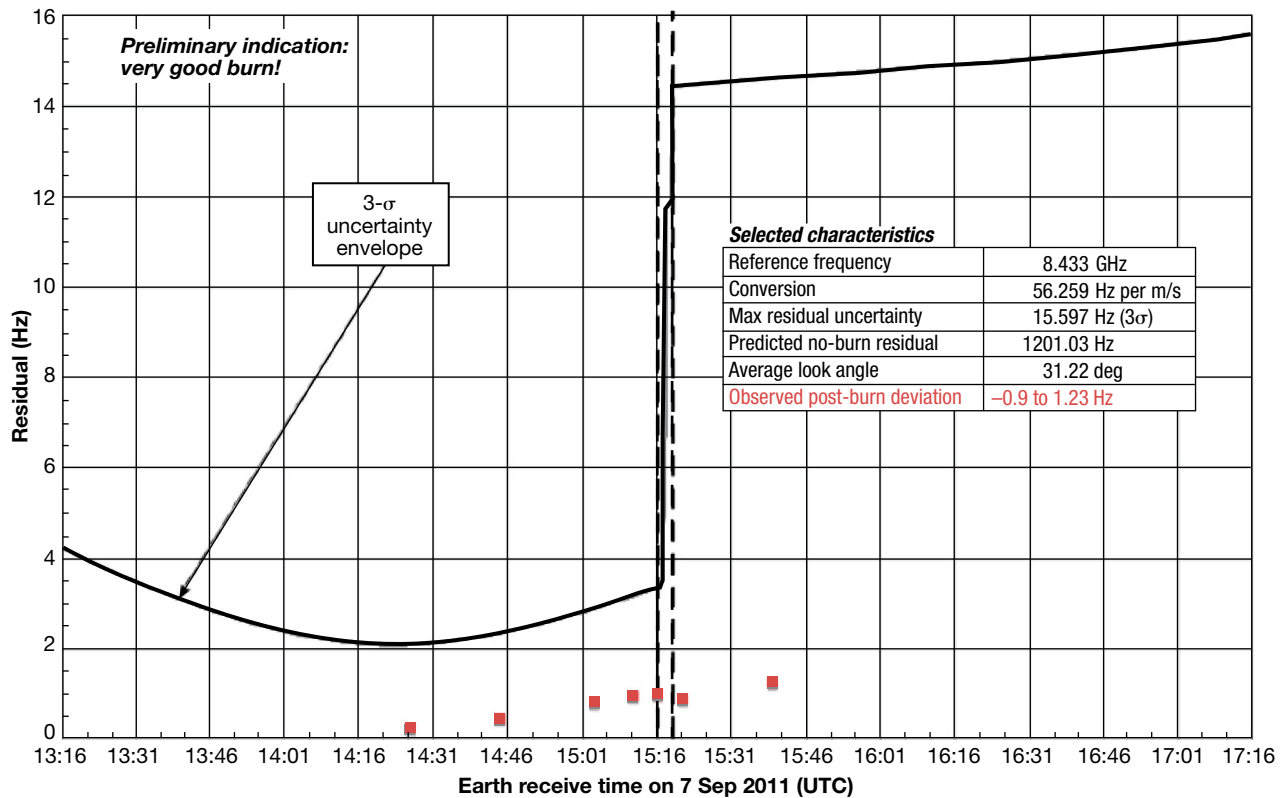
Figure 4. Real-time Doppler residual monitoring results for OCM-3. Measured Doppler residuals received before and after OCM-3 execution are represented by red squares at the bottom of the figure, and the OCM-3 active thrust time is indicated by the area between the closely spaced dashed lines.

cury environment. After Mercury flybys and MOI, the navigation team solved for a series of Mercury gravity field models, culminating in the model designated MNG04, which included tracking data from all three Mercury flybys, seven sidereal rotations of Mercury, and minimum altitudes down to 200 km. This spherical harmonic expansion to degree and order 20 was essential for accurate trajectory determination in the highly eccentric orbit around Mercury. In addition, accurate modeling and estimation of radiation pressure was important because of both Mercury's close proximity to the Sun and extreme dayside-to-nightside temperature variations on the spacecraft as it orbited Mercury. Table 5 lists estimated and considered parameters used in the orbit determination filter and required for accurate maneuver reconstruction. Table 6 lists targeted orbit characteristics for OCM-3, along with the navigation team's final post-OCM-3 orbit reconstruction.

A 200-Hz burn-time integration model developed during MESSENGER's flight was used to calculate propellant consumption from all tanks as a function of on time, feed pressure, and duty cycle using subsystem telemetry and thruster performance curves provided by Aerojet Rocketdyne. The burn-time integration model, however, was ill equipped to handle helium flow, and

updating legacy MATLAB and Simulink code originally designed to evaluate bipropellant maneuvers was considered an inefficient use of project resources. Therefore, starting with OCM-12, which was intended to evaluate thruster performance with GHe pressurant, a 1-Hz Excel model was developed. This model could change

Table 5. Estimated and considered parameters during the orbital mission phase

Estimated Parameters	Considered Parameters
Position and velocity	Station locations
Solar radiation pressure specular and diffuse reflectivity coefficients	Earth troposphere model parameters
Planetary radiation pressure specular and diffuse reflectivity coefficients	Earth ionosphere model parameters
Mercury albedo specular and diffuse reflectivity coefficients	Earth pole, UT1
ΔV due to commanded momentum dumps	Earth ephemeris
OCMs	
Mercury ephemeris	
Mercury gravity field (spherical harmonic expansion to degree and order 20)	

Table 6. OCM-3 targeted and reconstructed orbital characteristics

Initial Orbit Characteristic	Value	Target or OD229 Expected Value	Deviation
Orbit period (s)[a]	42341.14	42338.97	2.17
Periapsis altitude (km)	200.34	200.00	0.342
Semi-major axis (km)	10001.01	10000.98	0.027
Eccentricity	0.736	0.736	-3.59×10^{-5}
Inclination (°)[b]	83.09	83.10	-2.46×10^{-3}
Right ascension of ascending node (°)[b]	348.37	348.37	3.42×10^{-3}
Argument of periapsis (°)[b]	113.22	113.23	-5.86×10^{-3}
Periapsis latitude (°)[b]	65.83	65.83	4.94×10^{-3}
Periapsis crossing time (UTC)	21:03:13.8	21:03:12.0	1.75 (s)

[a] First to second post-MOI periapsis
[b] Inertial relative to Mercury true equator

propellant type mid-maneuver on the basis of observed thruster performance. Both models were also used before maneuvers to provide propellant usage predictions to the mission design and G&C teams.

Ideal gas or pressure–volume–temperature (PVT) relations, which account for propellant vapor pressure and pressurant compressibility, were used in parallel with both propellant consumption models to verify that observed pressure and temperature drops were consistent with expected propellant usage. The PVT model was also used to calculate remaining propellant in the AUX, although this approach was based on the assumption of a fixed helium load in the AUX. Only the PVT model was used to compute the helium mass expelled or transferred from all four tanks.

MONITORING AND FAULT PROTECTION

The MESSENGER avionics architecture included a main processor (MP) that ran the software for onboard command and data handling and G&C functionality. The avionics also included a pair of FPPs that ran identical flight software and ensured spacecraft health and safety. The dual-FPP approach provided redundancy in case one FPP failed (a single FPP could provide all necessary protection).

The FPP flight software used an onboard software-based autonomy engine, which provided a framework on which to build the spacecraft fault-protection system. Because the MESSENGER spacecraft was typically in contact with ground tracking stations for only a few hours per week, the autonomy engine was the primary line of defense for addressing spacecraft operational faults. The autonomy engine was a monitor-to-response system, with which faults were detected (*monitor*) and corrective actions were taken (*response*) to address faults. The autonomy engine supported autonomy rules and macros that could be uploaded to the spacecraft.

Autonomy rules defined the fault conditions to be monitored, such that each rule could access all onboard engineering telemetry (e.g., voltages, temperatures, currents, pressures, software counters and flags) to check for faults. The autonomy engine collected these data by monitoring all data interactions between the MP software and spacecraft components. For example, when the MP software read a star tracker's temperature, the FPP would "snoop" that transaction and make those sensor data available for evaluation in autonomy rules. The autonomy rules would define the fault conditions (e.g., star tracker temperature >20°C).

Macros defined a sequence of autonomously executed commands (such as power cycling a component, switching to a redundant component, or demoting the spacecraft into a safe mode) to address the fault. The interaction of autonomy rules, macros, and spacecraft components is shown in Fig. 5.

Before launch, a default set of autonomy rules and macros was loaded on the spacecraft, thereby enabling all planned fault protection. However, the design provided flexibility to allow autonomy objects to be added, modified, or deleted at almost any point during the mission. This flexibility allowed the fault-protection engineer to create customized monitors and responses to support specific events throughout the mission such as TCMs, OCMs, and MOI.
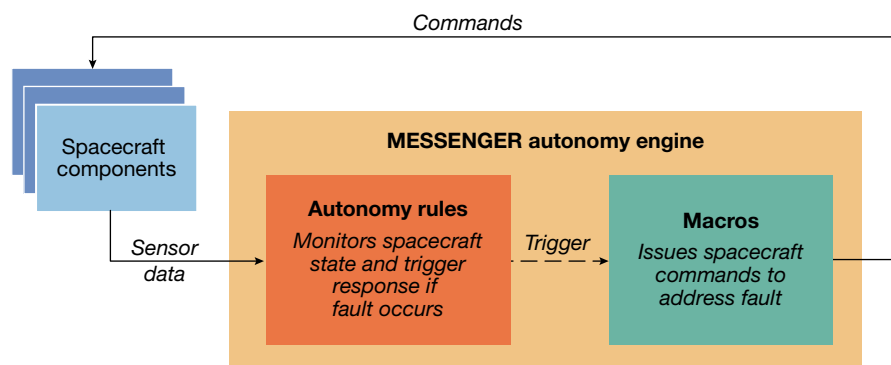

Figure 5. Process overview for MESSENGER autonomy.

Fault Protection for DSMs

For the five DSMs during cruise, the fault-protection system configuration was customized to maximize maneuver success while offering protection to address other faults. Detection of faults directly related to the performance of a maneuver was performed within the G&C flight software in the MP via the burn initiation and burn abort checks described earlier in the Maneuver Planning and Implementation section. Each check could be individually enabled or disabled depending on the characteristics of the maneuver. If a G&C burn abort check tripped during the maneuver, the G&C software would set a flag that the FPP monitored, and an autonomy rule would trigger a macro that would shut down the propulsion system to complete the maneuver abort.

For faults not monitored by the G&C software, the autonomy system would delay the macro response to most faults until after maneuver completion. For example, any telecommunications system fault during a maneuver would be detected and "latched," but the response would wait until the maneuver ended because the telecommunications system was not required to complete the maneuver. All five DSMs completed without any unexpected autonomy responses.

Fault Protection for MOI

Aside from launch, MOI was the mission's most critical event. As with DSMs, the detection of faults directly related to maneuver performance was performed by onboard G&C software through its burn initiation and burn abort checks. Faults not related to maneuvers had their responses delayed until after maneuver completion.

A unique challenge for MOI was the configuration of the fault-protection system in the hours before the maneuver started. In the event of a critical fault and safe-mode demotion before MOI, any planned onboard maneuver would not execute without ground segment team intervention, which would involve diagnosing the problem and restoring the spacecraft to its full operational state before MOI. Successful recovery from a critical fault could have been either challenging or impossible if that fault occurred hours or minutes before MOI.

To mitigate this risk, the 24 h before MOI were defined as *pre-MOI*. At the start of pre-MOI, the fault-protection system was configured to defer the response to most faults until after MOI completion (a 24-h maximum fault response delay). This decreased the chance that a fault with no effect on MOI would prematurely demote the spacecraft into a safe mode and prevent MOI execution. Before MOI, the spacecraft was in continuous contact with ground operators, thereby enabling real-time corrective action if a fault was observed. For the actual MOI event, the fault protection was nominal for the entire pre-MOI and MOI with no unexpected faults.

Fault Protection for OCMs

During the 19 OCMs executed during the 4 years in orbit, the fault-protection system once again provided customized spacecraft protection with a focus on which propellant tanks were used for each maneuver. For OCMs near the mission's end, propellant conservation was key to meeting the science goals. Because of uncertainty in how much usable propellant remained, autonomy rules and macros were added to detect a sufficiently large pressure drop in the fuel tanks during the maneuver to indicate propellant depletion and to close fuel tank latch valves and open the AUX latch valve to allow the OCM to continue. This capability aided the mission in maximizing the use of available propellant without *a priori* knowledge of the available propellant in each tank.

PROPULSION SYSTEM MANAGEMENT FOR MANEUVERS

Before MESSENGER's launch, it was expected that the propellant in the main tanks would return to the center of the tanks after ΔV maneuvers, providing a predictable center of mass and allowing for passive momentum management with spacecraft sunshade tilting. However, the spacecraft angular momentum magnitude increased faster than expected after DSM-1, far faster than the passive technique could countermand. As a result, a commanded momentum dump with the thrusters was required. Subsequent analysis[6] indicated that, because of surface tension forces causing propellant to adhere to the annular baffles in the main propellant tanks, the propellant remained at the outlet end of the tanks after DSM-1. This issue was ultimately resolved when the team devised a new spacecraft attitude alternation (and solar-array articulation) strategy heading into the first Mercury flyby. From that point through the MOI maneuver, momentum dumps were no longer required and DSMs could be executed purely with z-direction thrust (Fig. 1).

With only ~13% of the original main fuel tank load and ~3% of the original oxidizer load remaining after MOI, extracting propellant became a challenge. The

Table 7. Nominal post-MOI LVA burn sequence

Segment No.	Burn Type	Thruster(s)	Minimum Duration (s)	Propellant Source
1	Settle	A1, A2, B1, B2	60	AUX
2	Settle/refill	C1 and C4 or C2 and C3	23	Main tanks
3	Main	LVA	12	Main tanks
4	Trim	C1 and C4 or C2 and C3	61	Main tanks

two annular baffles proved to be problematic at low propellant fill fractions. Use of the standard thruster firing routines would cause a substantial amount of propellant to splash onto the baffles and adhere to the upper and lower sides because of surface tension. In addition, the unconstrained slosh of the remaining propellant would lead to intermittent and unpredictable periods of gas flow to the thrusters. To avoid these scenarios, optimal thruster operation and tank-switching strategies were developed that would both minimize propellant lost to the baffles and prevent gas ingestion to the thrusters.[3] As an example, the minimum durations, primary thrusters, and propellant source(s) for each segment used in OCM-1 and OCM-3 appear in Table 7. Depending on the thrusters and tanks designated for use, multiple sequences were developed to maximize remaining propellant during other OCMs. Durations and propellant source(s) for OCM-9 appear in Table 8. The propulsive rationale for each segment follows:

Segment 1: *Settling.* 60-s A/B thruster minimum: to move as much propellant as possible off of each tank's lower baffle toward the tank outlet with A/B-only thrust.

Segment 2: *Settle/refill.* 23-s two-C-thruster minimum: to make the propellant sufficiently quiescent that LVA ignition would not cause a geyser that reached beyond the bottom baffle. "Refill" moved N_2H_4 from FT1 or FT2 to AUX for later use.

Segment 3: *Main.* 12-s LVA minimum: to dampen the propellant excitation from initial LVA ignition sufficiently so that, upon LVA shutdown, the sudden loss of force would not cause a propellant geyser to reach beyond the bottom baffle.

Segment 4: *Trim.* 61-s two-C-thruster minimum: to further stabilize the propellant after LVA shutdown.

A "tweak" segment, not shown in Tables 7 or 8, ended every MESSENGER maneuver.[1] The tweak segment began when the ΔV thrusters were disabled and the attitude-control thrusters continued firing to allow structural excitations and propellant slosh to damp out before returning control to the reaction wheels. Tweak segments typically employed very low duty cycles and consumed a negligible amount of propellant.

Table 8. Operational guidelines for FT1 and FT2 propellant mass <7.35 kg

Segment No.	Burn Type	Thrusters	Minimum Duration (s)	Propellant Source
1	Settle	A1, A2, B1, B2	60	AUX
2	Main	C1 and C4 or C2 and C3	35	First 40 s: AUX; after 40 s: FT1/FT2
3	Trim	A1, A2, B1, B2	50	If Main <40 s: AUX; if Main >40 s: FT1/FT2

Table 9. GHe load at BOL, before OCM-15A, and EOL

Tank	BOL Load (kg) before Launch	Usable Load (kg) before OCM-15A	Usable Load (kg) before Impact
Helium	2.270	0.539	0.081
AUX	0.017	0.029[a]	0.000
FT1	0.062	0.636	0.227
FT2	0.062	0.587	0.204
Oxidizer	0.058	0.000	0.000
Total	2.469	1.791	0.512

[a] 0.017 kg on inaccessible side of diaphragm

Remaining N_2O_4 in the oxidizer tank was never accessed after the final dual-mode burn OCM-7.[3] After OCM-15, no hydrazine decomposition was observed on any maneuver's primary thrusters, indicating that all fuel tanks were empty of usable N_2H_4. Starting with OCM-15A, all remaining maneuvers used GHe as a cold gas propellant through the monopropellant thrusters. Table 9 shows the helium loads at BOL and EOL. After OCM-18, 0.512 kg of usable GHe remained. At a prior-to-impact feed pressure of 710 kPa (103 psi), capacity for further delivered GHe thrust was limited.

MERCURY ORBIT INSERTION

Postlaunch Changes in MOI

With MESSENGER being the first spacecraft to orbit the planet Mercury, the mission's most important maneuver imparted the largest velocity change. This orbit-insertion maneuver slowed the spacecraft sufficiently to place it into orbit around Mercury. The primary science orbit at the start of science data collection was to have a 200-km minimum altitude, a 12-h orbit period, an 80° orbit inclination, and a 60°N subspacecraft periapsis latitude. The orbit design had an additional requirement that aligned the line between the spacecraft's two Mercury equator crossings to be close to orthogonal to the Mercury–Sun direction at Mercury perihelion. Well before DSM-5 in November 2009 (the final opportunity to make large changes to the geometry of MESSENGER's arrival at Mercury), the science team worked with the mission design and navigation teams to arrive at a new 82.5° initial orbit inclination (±1°).[7] Propagation of the spacecraft orbit for 1 year after MOI indicated that orbit inclination could increase to 84.1°, which could approach the science team's maximum allowable 85° inclination during the orbital phase if a 1° maximum inclination error occurred at MOI. This 2.5° increase in the spacecraft's orbit inclination at Mercury permitted key observations of polar deposits on the permanently shadowed floors of near-polar craters that would have been more difficult at an 80° initial orbit inclination.

Another major postlaunch change to MOI was a shift from two maneuvers to a single maneuver. Development of the SciBox science operations planning software enabled a loosening of the initial orbit period tolerance from ±1 min to ±10 min (see Ensor et al., this issue). This change in orbit period tolerance enabled mission planners to save propellant and lessen risk by using a less-precise single MOI maneuver. The earlier plan to begin with a 96%-of-total-MOI ΔV bipropellant maneuver followed 3.6 days later by a precise 4% ΔV follow-up maneuver would have been needed only to satisfy the tighter orbit period tolerance. A complete history of the changes to and performance of MESSENGER's MOI has been provided by McAdams et al.[8]

Preparing for nominal and contingency aspects of MOI involved using two of six bipropellant maneuvers (one of five DSMs was split into two parts) to test maneuver features that were uniquely required for MOI. Three years before MOI, DSM-3 tested a constant rate of change in the thrust direction, a requirement of MOI to orient the thrust vector nearly opposite to the instantaneous Mercury-relative spacecraft velocity direction. This DSM-3 closed-loop test of an MOI variable-thrust direction requirement lessened risk by shifting this first-use requirement from MOI to a less critical TCM with 92% less ΔV than would have been required at MOI. A December 2008 DSM-4 open-loop test of MOI's variable-thrust direction (turn rate) without using accelerometer data yielded a successful ΔV with a larger error in ΔV magnitude and direction than experienced during DSM-3. With DSM-4 split into two parts at a 9:1 ratio and the open-loop, no-accelerometer contingency on the smaller component, mission planners minimized mission risk and increased confidence in successful MOI execution if accelerometer function had been inadvertently suspended during that 14- to 15-min maneuver.

Performance of MOI

Between the August 2009 MOI preliminary design review and the March 2011 final MOI implementation adjustments, several refinements improved MOI performance. One refinement involved changing arrival target parameters to account for the change from two MOI maneuvers to one MOI maneuver. A second refinement shifted MOI initial thrust time to (i) minimize ΔV and (ii) account

for actual time drift from spacecraft perceived time associated with extended operation using the onboard coarse oscillator. A third refinement incorporated the most detailed propulsive performance model available during the first 2 min of LVA thruster firing, a time before thrust magnitude and specific impulse settled into steady-state fixed values. For example, six polynomial curve fits modeled thrust magnitude variations from 709 N to 683.5 N and corresponding variations in specific impulse that occurred with fuel tank switches every 20 s to control center-of-gravity location. A fourth refinement, updating the solar and planetary ephemerides from the 2001 basis de405 to the 2010 update de423, reduced the uncertainty in the time-dependent position of Mercury relative to MESSENGER by 1–2 km. The de423 ephemeris included improvements in Mercury's orbital position and velocity derived from MESSENGER's three Mercury flybys in 2008 and 2009.

Orbit-insertion performance margins were greater than the target offsets observed in the reconstruction of the final MOI maneuver and initial Mercury orbit. With the MOI velocity direction aligned such that the Sun direction would stay within 8° of the normal to the sunshade center panel, the observed 9.6° upper limit during MOI fell below the 12° constraint that keeps direct sunlight from reaching sensitive spacecraft components. As evident from Fig. 6, the entire MOI maneuver was directly observable from Earth with DSN antennas in Goldstone (California) and Canberra (Australia), each able to observe the MESSENGER spacecraft more than
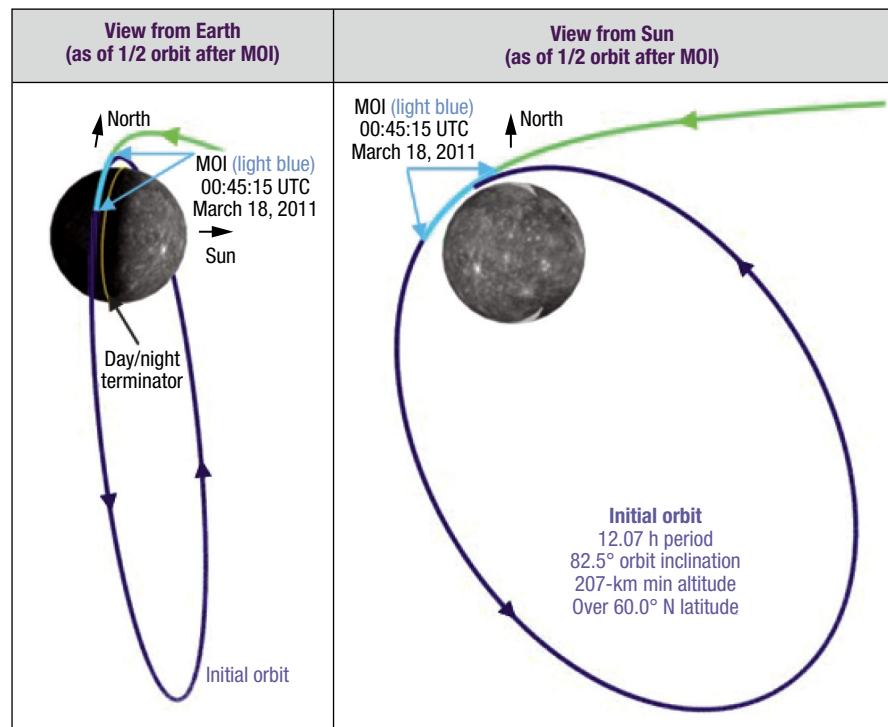
View from Earth
(as of 1/2 orbit after MOI)

North

MOI (light blue)
00:45:15 UTC
March 18, 2011

Sun

Day/night terminator

Initial orbit

View from Sun
(as of 1/2 orbit after MOI)

MOI (light blue)
00:45:15 UTC
March 18, 2011

North

Initial orbit
12.07 h period
82.5° orbit inclination
207-km min altitude
Over 60.0° N latitude

Figure 6. Two views of MESSENGER's orbit insertion and initial orbit around Mercury.

Table 10. Key performance results for MOI

	Orbit Period (h)	Minimum Altitude (km)	Orbit Inclination (°)	Mercury Latitude (°N) at Minimum Altitude	ΔV along Path (m/s)
Target	11.999	200.00	82.500	60.000	862.166
Result	12.071	206.77	82.522	59.976	861.714
Error	+0.072	+6.77	+0.022	–0.024	–0.452
3-σ tolerance[a]	±0.167	±20.00	±1.000	±2.000	N/A

[a] σ denotes standard deviation.

30° above the horizon. Table 10 provides an assessment of key MOI performance parameters for the initial orbit around Mercury and the MOI maneuver, for which the total integrated velocity change direction differed by <0.5° from that in the baseline plan.

The navigation team provided the final assessment of MOI ΔV and post-MOI orbit determination. The measure used to judge the accuracy of the approach to a planetary flyby or orbit insertion is the target planet intercept point in the hyperbolic impact-plane, or B-plane. The B-plane is the plane normal to the incoming asymptote of the hyperbolic flyby trajectory that passes through the center of the target body. The "S axis" is in the direction of the incoming asymptote and hence is normal to the B-plane. For MESSENGER, the "T axis" was parallel to the line of intersection between the B-plane and the Earth Mean Ecliptic plane of 1 January 2000 and was positive in the direction of decreasing right ascension. The "R axis," positive toward the south ecliptic pole, completes the mutually orthogonal right-handed Cartesian coordinate axes "T-R-S." This B-plane definition appears in Fig. 7.

The evolution of the 3-standard-deviation dispersion ellipse for the final operational orbit determination solutions before MOI is shown in Fig. 8, along with the final reconstructed ellipse derived from post-MOI radiomet-
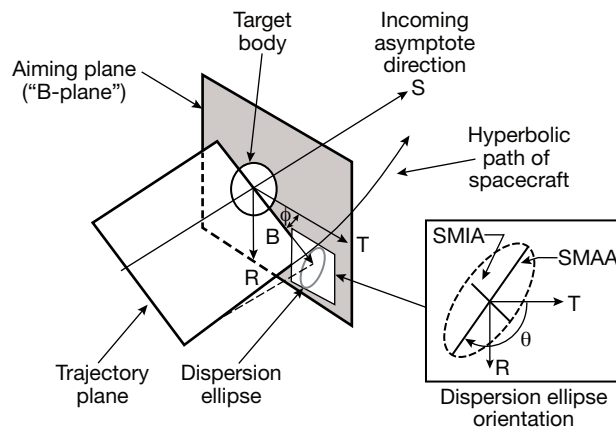
ric tracking data. The error ellipse size in the B-plane decreases as time to closest approach decreases. Leading up to MOI, the size and predicted location of the error ellipse varied because of a number of factors, including uncertainty in solar radiation pressure modeling and the effect of a superior solar conjunction ~2 weeks before MOI. The navigation team recommended that solar-sailing parameters be adjusted to move the predicted aimpoint several kilometers closer to the nominal target, but there was some reluctance to make changes to onboard sequences so close to MOI. As shown in Fig. 8, the final location of the trajectory in the B-plane was only ~8 km from the ideal target at MOI (~1 km of which is attributable to Mercury ephemeris error and 7 km of which was evident as periapsis altitude offset). This offset was within the previously determined predicted 3-standard-deviation dispersion and well within requirements for a successful orbit insertion.

Contingency Preparations for MOI

Before MOI, substantial effort was invested in order to prepare a recovery plan that would overcome virtu-
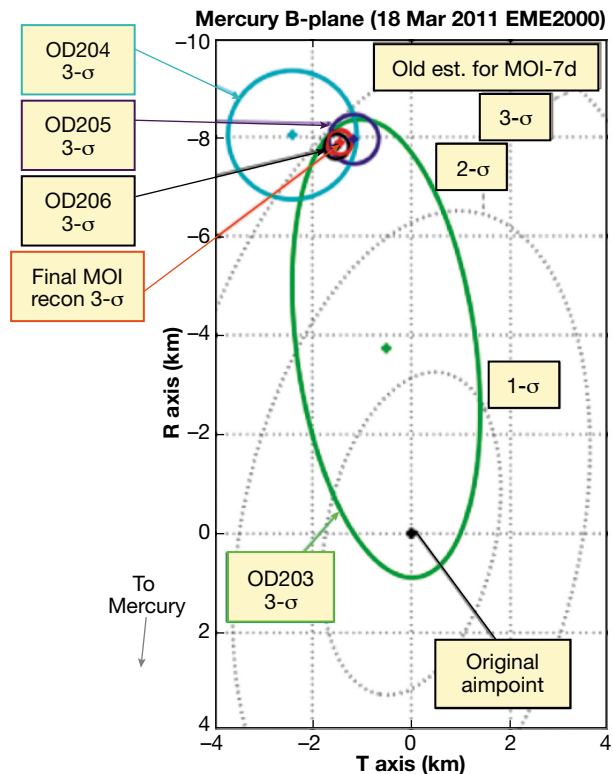

Figure 7. Definition of B-plane and error ellipse. SMAA, semi-major axis; SMIA, semi-minor axis.

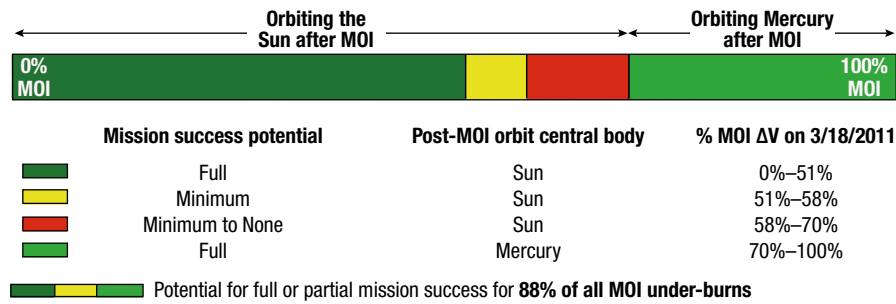**Figure 8.** MOI B-plane reconstruction.

Figure 9. Recovery outlook for MOI underburn options.

ally any MOI anomaly. With almost no possibility for an MOI overburn exceeding 1% in ΔV magnitude, the MOI contingency recovery analysis focused on recovery from heliocentric orbit if <70% of the MOI ΔV was imparted as well as recovery from high Mercury orbit for underburns of <30%. The recovery options were developed with a maximum MOI delay of 5 years and trajectories that required as many as seven extra Mercury flybys between an anomalous MOI/Mercury flyby and the delayed MOI. For recovery from loosely captured orbits around Mercury, one or two carefully timed maneuvers after MOI would have been needed to establish the primary science orbit. Some of the identified recovery scenarios were complicated, with features such as retrograde inclination orbits, solar conjunction avoidance, eclipse avoidance, and maneuver delays to accommodate the SKI sunshade orientation constraint. Figure 9 provides an overview of the prospects for MOI anomaly recovery to either full-mission success or partial-mission success. Among multiple formally defined success criteria was the time orbiting Mercury, with minimum requirements of 1 year for full-mission success and 90 days for partial-mission success.

CONCLUSION

Key factors to MESSENGER's mission success included successful, on-time maneuver implementation and substantial propellant margin for extended-mission operations. The flight team repeatedly made alterations to original maneuver design and implementation procedures in order to accommodate changes in science requirements or maximize the amount of usable propellant. This operational flexibility resulted from close coordination among the mission systems engineer and the science, mission design, G&C, propulsion, navigation, autonomy, and mission operations teams. Despite the large number of variations from the maneuver implementation modes known before launch, the flight team never deviated from their practice of minimizing overall functional risk to the spacecraft and science instruments. Repeated coordination of these elements of MESSENGER flight operations elevated confidence in successful operation during the higher-risk, low-minimum altitude final mission extension.

REFERENCES

[1]Wiley, S. R., Dommer, K., and Mosher, L. E., "Design and Development of the MESSENGER Propulsion System," in *Proc. 39th AIAA/ASME/SAE/ASEE Joint Propulsion Conf. and Exhibit*, Huntsville, AL, paper AIAA-2003-5078, pp. 1–20 (2003).

[2]Wilson, M. N., Engelbrecht, C. S., and Trela, M. D., "Flight Performance of the MESSENGER Propulsion System from Launch to Orbit Insertion," in *Proc. 48th AIAA/ASME/SAE/ASEE Joint Propulsion Conf. and Exhibit*, Atlanta, GA, paper AIAA-2012-4333, pp. 1–23 (2012).

[3]Wilson, M. N., Engelbrecht, C. S., and Jaekle, D. E., "MESSENGER Propulsion System: Strategies for Orbit-Phase Propellant Extraction at Low Fill Fractions," in *Proc. 49th AIAA/ASME/SAE/ASEE Joint Propulsion Conf. and Exhibit*, San Jose, CA, paper AIAA-2013-3757, pp. 1–15 (2013).

[4]Tam, W., Wiley, S. R., Dommer, K., Mosher, L. E., and Persons, D., "Design and Manufacture of the MESSENGER Propellant Tank Assembly," in *Proc. 38th AIAA/ASME/SAE/ASEE Joint Propulsion Conf. and Exhibit*, Indianapolis, IN, paper AIAA-2002-4139, pp. 1–17 (2002).

[5]Stanbridge, D. R., Williams, K. E., Taylor, A. H., Page, B. R., Bryan, C. G., Dunham, D. W., Wolff, P., Williams, B. G., McAdams, J. V., and Moessner, D. P., "Achievable Force Model Accuracies for MESSENGER in Mercury Orbit," in *Astrodynamics 2011: Part III, Advances in the Astronautical Sciences*, Vol. 142, Univelt, San Diego, pp. 2231–2249 (2012).

[6]O'Shaughnessy, D. J., Vaughan, R. M., Chouinard, T. L. III, and Jaekle, D. E., "Impacts of Center of Mass Shifts on MESSENGER Spacecraft Operations," in *Proc. 20th International Symp. on Space Flight Dynamics*, Annapolis, MD, paper 12-4, pp. 1–15 (2007).

[7]Page, B. R., Williams, K. E., Taylor, A. H., Stanbridge, D. R., Bryan, C. G., Wolff, P. J., Williams, B. G., O'Shaughnessy, D. J., and Flanigan, S. H., "Applying Experience from Mercury Encounters to MESSENGER'S Mercury Orbital Mission," *Astrodynamics 2011: Part III, Advances in the Astronautical Sciences*, Vol. 142, Univelt, San Diego, pp. 2250–2269 (2012).

[8]McAdams, J. V., Bryan, C. G., Bushman, S. S., Calloway, A. B., Carranza, E., Flanigan, S. H., Kirk, M. N., Korth, H., Moessner, D. P., O'Shaughnessy, D. J., and Williams, K. E., "Engineering MESSENGER's Grand Finale at Mercury – The Low-Altitude Hover Campaign," in *Proc. AAS Astrodynamics Specialist Conf.*, Vail, CO, paper AAS 15-634, pp. 1–20 (2015).

James V. McAdams, KinetX Aerospace, Inc., Tempe, AZ

James V. McAdams, now working for KinetX Aerospace, concluded his MESSENGER responsibilities as a member of the Principal Professional Staff in the Astrodynamics and Control Systems Group in APL's Space Exploration Sector. He led the MESSENGER mission design team throughout mission conceptual studies and all mission phases. His e-mail address is jim.mcadams@kinetx.com.

Carl S. Engelbrecht, Space Exploration Sector, Johns Hopkins University Applied Physics Laboratory, Laurel, MD

Carl S. Engelbrecht is a member of the Principal Professional Staff in APL's Space Exploration Sector. He is the lead propulsion engineer for the Europa Project and was the lead propulsion engineer for MESSENGER from before launch until after MOI. His e-mail address is carl.engelbrecht@jhuapl.edu.

Christopher G. Bryan, KinetX Aerospace, Inc., Tempe, AZ

Christopher G. Bryan is a member of the Space Navigation and Flight Dynamics group at KinetX Aerospace. He was a navigation team chief for MESSENGER as well as a member of the New Horizons navigation team for the flyby of Pluto. His e-mail address is chris@kinetx.com.

Sarah H. Flanigan, Space Exploration Sector, Johns Hopkins University Applied Physics Laboratory, Laurel, MD

Sarah H. Flanigan is a member of the Senior Professional Staff in APL's Space Exploration Sector. She specializes in spacecraft G&C and served as the lead G&C engineer during the last 3 years of the MESSENGER mission. Her e-mail address is sarah.flanigan@jhuapl.edu.

Stewart S. Bushman, Space Exploration Sector, Johns Hopkins University Applied Physics Laboratory, Laurel, MD

Stewart S. Bushman is supervisor of the Propulsion Section in APL's Space Exploration Sector Mechanical Systems Group. He is the propulsion lead engineer for the MESSENGER, Solar TErrestrial RElations Observatory, New Horizons, and Parker Solar Probe missions. His e-mail address is stewart.bushman@jhuapl.edu.

T. Adrian Hill, Space Exploration Sector, Johns Hopkins University Applied Physics Laboratory, Laurel, MD

T. Adrian Hill is a member of the Principal Professional Staff in APL's Space Exploration Sector. He is currently leading the development of the autonomy system for the Parker Solar Probe mission and led the development of flight software for MESSENGER. His e-mail address is adrian.hill@jhuapl.edu.